International Journal of Thin Films Science and Technology

http://dx.doi.org/10.12785/ijtfst/040210

Thin Films of TiO_2-MoO_3 Binary Oxides Obtained by an Economically Viable and Simplified Spray Pyrolysis Technique for Gas Sensing Application

*V. Sivaranjani, P. Deepa and P. Philominathan**

PG and Research Department of Physics, AVVM Sri Pushpam College (an autonomous institution affiliated to Bharathidasan University, Trichy), Poondi, Thanjavur 613 503, India.

Received: 18 Feb. 2015, Revised: 6 Apr. 2015, Accepted: 7 Apr. 2015.
Published online: 1 May 2015.

Abstract: Thin films of binary oxides (TiO_2-MoO_3) of varied molar concentrations of MoO_3 (from 0.15 M to 0.30 M insteps of 0.05 M) have been prepared by a simplified and cost effective perfume atomizer technique on quartz substrates at 500˚C. To investigate the structural, morphological, photoluminescence, optical and gas sensing properties of as-deposited films, the characterization studies using X-ray diffraction(XRD), scanning electron microscope(SEM) and Ultraviolet-Visible-Near infrared (UV-Vis-NIR) and photoluminescence(PL) spectroscopy were utilized. The structural analysis confirmed that the films were polycrystalline with rutile and orthorhombic phase types pertain to TiO_2 and MoO_3 crystal structures. All the samples exhibited very poor optical transmission in the entire region of UV-vis-NIR and the optical band gap was increased as increase in MoO_3 concentration. The variation in intensity of Photoluminescence (PL) emission was also found to occur while varying the concentration. The images of SEM showed structures of spherical grains with minimal distribution and flower like formations for varied concentrations. The gas sensing ability of these films was also demonstrated in 100 ppm of ethanol vapour at room temperature and the enhanced sensitivity was found in Q3 sample.

Keywords: Binary oxides; Gas sensor; XRD; Perfume atomizer method.

1 Introduction

The search for metal oxide compounds have been phenomenal in recent times due to their applicability in various fields extensively and in particular, gas sensing applications [1-4]. Among varieties of metal oxides, a few like CuO_2, MoO_3, WO_3, SnO_2, In_2O_3 etc., were identified as suitable candidates for gas sensing applications. More specifically, in gas sensing applications, certain materials which satisfy the essential necessities such as reliability, readiness, stability and low cost; are preferred and hence, play crucial role and hold the key in academic research and industry. As a consequence, the metal oxide semiconductor (MOS) thin films have been traditionally used as gas-sensors and also, the invasion of TiO_2 metal oxide films in photo-electrochemical solar cells, photo-catalysis, gas sensors, interference filters, capacitor etc., [5] have created a wide and growing interest in recent years. In particular, the oxidation affinity, stability and non-toxicity of TiO_2 have intensified the research on multiple applications like dielectrics in memory cell capacitors, semiconductor field effect transistors, anti-reflection coatings, multilayer coatings and optical waveguides etc., [6-10]. Further, as the titanium oxides have large band gaps, play a deep role in developing various environmental and energy related applications [11].

Hence, in the recent past, many researchers have explored the possibility of enhancing the properties of TiO_2 when mixed with certain transition metal ions like F, Mo, Sb, V, W, etc., [12-14] to a larger extent. Interestingly, the molybdenum oxide has been found to be a one of the metal oxide semiconductors which has promising gas sensing ability as well as certain unique optical properties. As for MoO_3, it has two problems for gas sensing, which are (i) It has a low evaporating temperature, so it permitting only low operating temperatures, however such temperature may not indeed be the optimal working temperature for particular gas species. (ii) The material has a very high resistivity, making it a difficult material to realize as a gas sensor and to integrate with electronics. Although, these two disadvantages have been identified, MoO_3 possesses good gas response since it has been used in the field of catalysis for oxidation reactions of hydrocarbons [15]. Moreover, the catalysts are used to increase the chemisorptions process and instigate fast response as well as high sensitivity and improved selectivity. TiO_2 was mixed with pure MoO_3 system and hence it would decrease the film resistivity and to promote

*Corresponding author e-mail: philominathan@gmail.com

improved gas sensing characteristics of pure MoO_3. The gas sensing properties of binary and mixed TiO_2-MoO_3 was reported by fabricating sol-gel and sputtering techniques [16-17]. Following the pursuit of probing this binary oxide film, though many conventional techniques for fabricating MOS thin film gas sensors were employed already, in this present study, we intend to employ yet another simplified technique, namely, a simplified spray pyrolysis method using perfume atomizer. Apart from simplicity, low-cost alternative and financially beneficial compared to maintaining CVD or PVD techniques, this method is flexible for process modifications, large area thin films, and vacuum free and high portability.

2 Materials and methods

As suggested by Sawada et al and others [18-20], the experiments were carried out in a ceramic walled chamber equipped with Kanthal heating resistance wire based base plate, capable of having temperature control ranging from room temperature to 700˚C. To start with, $TiCl_4$ (source of TiO_2) was dissolved in 5ml of ethanol and $MoCl_5$ (starting material of MoO_3) in 10 ml of ethanol and mixed together. Then, this mixture of both the starting materials was stirred for a couple of hours and coated manually on thoroughly cleaned (with no contamination) quartz substrates using a perfume atomizer method; however, the temperature during the spray deposition was kept at 500˚C. The optimum deposition temperature to obtain crystalline binary oxide thin films is found to be 500˚C otherwise the films will exhibit amorphous nature as reported in [21].The molar concentration of TiO_2 was kept 1 M throughout the deposition process and MoO_3 is taken as 0.15 to 0.30 M in steps of 0.05 M (the prepared samples are labeled as Q1, Q2, Q3 and Q4).

The binary oxide films (TiO_2-MoO_3) were characterized by X-ray diffraction, UV-Visible-near infrared spectroscopy, photoluminescence spectroscopy and scanning electron microscope. The X-ray diffraction patterns were obtained using the computer controlled Phillips X'pert PRO XRD system (Cukα radiation λ=1. 5405 Å) in the Bragg-Brentano geometry. The Joint Committee on Powder Diffraction Standards (JCPDS) database from the International Centre for Diffraction Data (ICDD) was utilized for the identification of crystalline phases. The optical transmittance was measured using UV-Visible-NIR spectrometer (Perkin Elmer Lamda 35). The data analysis and optical properties modeling were performed using PUMA software [22]. The morphological studies of the samples were performed by scanning electron microscope (Hitachi, Model: S-3400N). The photoluminescence were carried out by spectrofluorometer (Jobin Y von-FLUROLOG FL3-11). The thicknesses of the samples were estimated by the weight gain method. Gas sensing characterization was carried out for 100ppm of ethanol concentration at room temperature with home-made testing chamber of 5L capacity.

3 Results and Discussion

3.1. X-ray diffraction studies

The X-ray diffraction patterns of TiO_2-MoO_3 binary oxide thin films as shown in Fig. 1, it is evident that the coexistence in a polycrystalline structure of TiO_2 and MoO_3 phases, as assigned according to standard diffraction data (JCPDS card No., 00-001-1292 (TiO_2), 00-005-0507 (MoO_3)). From the diffraction patterns, the binary oxide films show strong and high intensity peaks corresponding to (1 1 0) and (0 4 0) planes of rutile TiO_2 and orthorhombic MoO_3 crystal structure; along with a few weak intensity peaks correspond to (0 2 0), (1 1 0) and (1 5 0) reflection of MoO_3. In general, the diffraction peaks over the higher concentration samples are slightly sharper and stronger than those of lower concentration samples, indicating the fact that an increase in crystallinity of the deposited films strongly depends on molar concentration. It is also notable that the (1 1 0) and (0 4 0) peaks become more intense and sharper as an increase in concentration of MoO_3. It means that the crystallinity of the films have improved a bit and also the grain size has become larger with increasing the concentration of the binary oxide thin films.

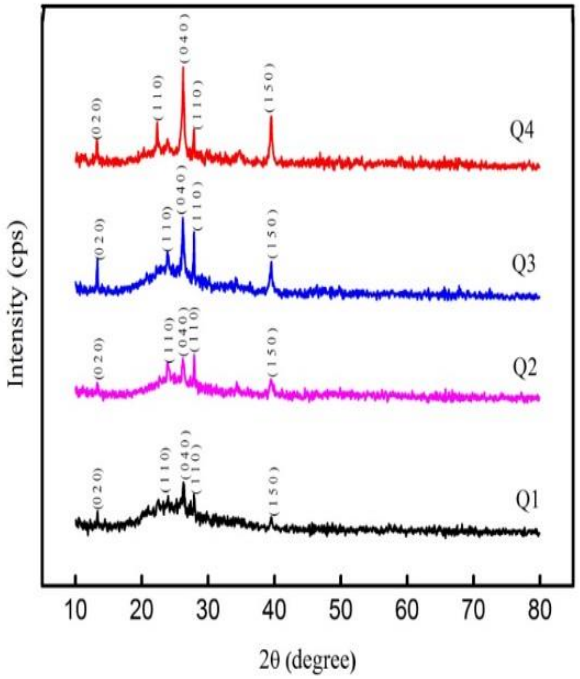

Fig.1. XRD patterns of TiO_2-MoO_3 binary films.

From XRD studies, the grain size was calculated using the full width half maximum (FWHM) of the high intensity diffraction peak according to Scherrer formula. It was found that the grain size seems to increase for the decrement in FWHM. Also, the thickness of the samples seems to increase (Q1 = 122 *nm*, Q2 = 179 *nm* Q3 = 422 *nm* and Q4 = 771 *nm*), as the average grain size of the TiO_2-MoO_3 thin films were found to increase with increase in concentration

as seen in Fig. 2. For instance, Q4 sample has shown its' thickness around 770 *nm* while the grain size is around 90 *nm*.

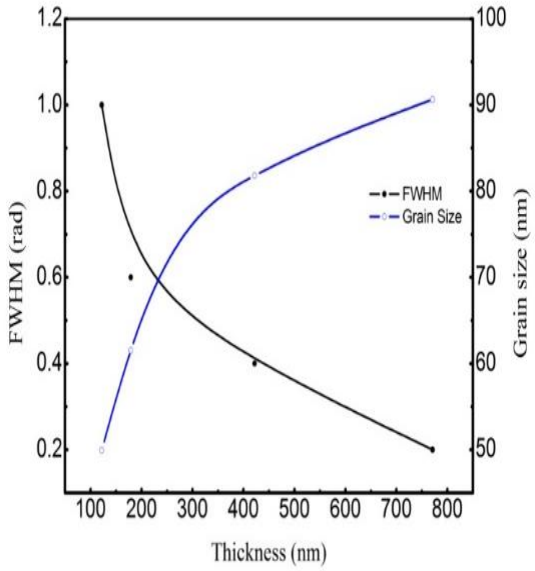

Fig. 2 Variation of FWHM and grain size of TiO_2-MoO_3 binary films as a function of film thickness.

3.2. Optical Studies

Fig. 3(a) shows the variation of transmission spectra of TiO_2-MoO_3 binary oxide thin films as a function of concentration level in the wavelength range of 350-1100 *nm*. All the films show poor transmittance behavior in the entire region of 350–1100 *nm*. Comparatively, only the sample Q1 and Q4 exhibited a maximum transmittance of ~25% in 1100 *nm*. The transmittance spectrum shows that the transmittance of Q2, Q3 and Q4 samples are lesser than that of Q1 sample. (The Q2,Q3 sample shows have lower transmittance compare to Q1 sample). However, the decrease in the optical transmittance of the binary films can be due to more electron scattering and ionized impurity scattering at a higher carrier concentration besides decrease in the solubility limit of Mo in the TiO_4 matrix, leading to increase of lattice distortion in some regions [23] and another reason for this decrement of transmittance was due to the maximum of light get reflected from these samples as depicted in refection spectrum shown in Fig. 3(c). Also, a maximum value of absorption co-efficient was found in Q1 samples compared with other higher concentration films such as Q2, Q3 and Q4, which is displayed in Fig. 3(b).

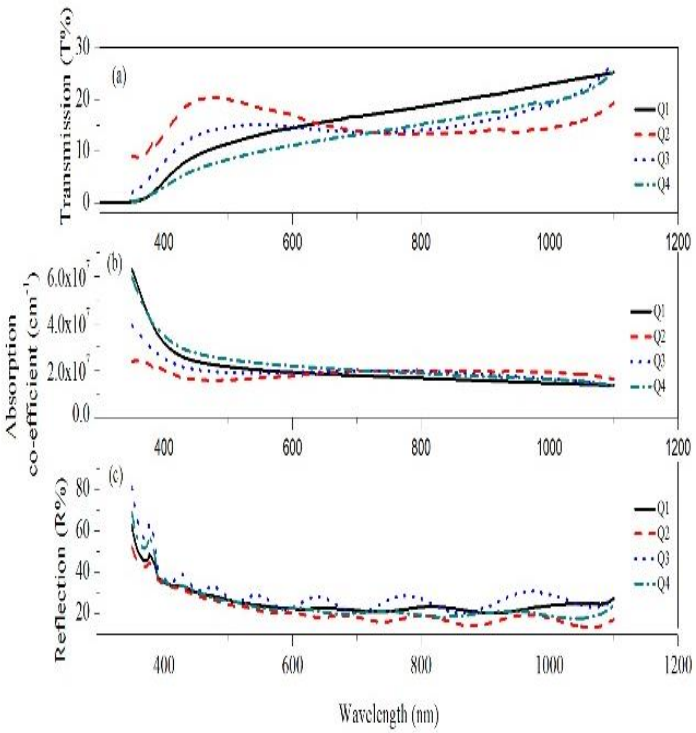

Fig.3.(a)Transmission (b)Absorption coefficient (c) Reflection Vs wavelength of TiO_2-MoO_3 binary films.

Moreover, a blue shift in the absorption edge was observed in figure 3(a). Which can be ascribed to the transition from the conduction band minimum (CBM) to an energy level below the valance band maximum (VBM), while the direct CBM-VBM transition is parity forbidden. The optical band gap can be determined using the Tauc's relationship [24] have been applied in a high absorbance region of the transmittance spectra and from the plot of $(\alpha h\upsilon)^2 Vs$ $(h\upsilon)$, deduced 2.6 *eV* for Q1, 2.7 *eV* for Q2, 2.9 *eV* for Q3 and 3.2 *eV* for Q4. It is obvious that as the concentration increases the band gap gets increased; the increment of band gap was due to Burstein-Moss effect, according to Burstein-Moss effect, raising the Fermi level into the conduction band of degenerate semiconductor leads to energy band broadening. Further, the index of refraction in the wavelength region (300-1100 *nm*) of the binary oxide thin films was estimated employing the PUMA software [22] and shown in Fig. 4.

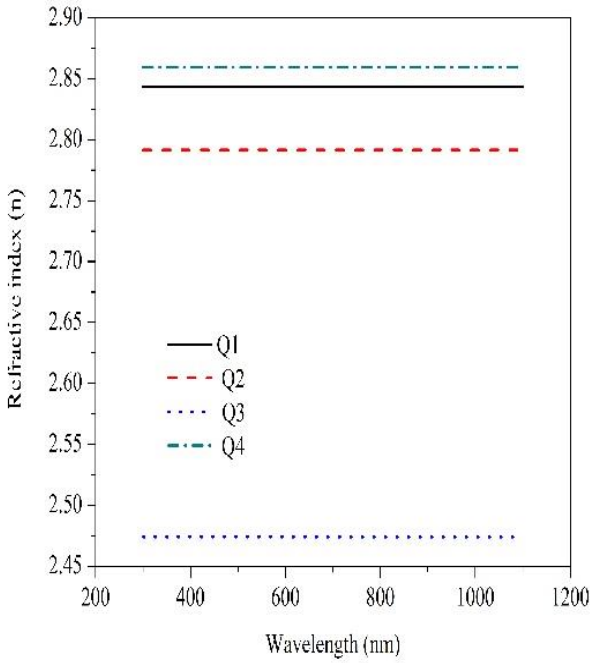

Fig. 4. Refractive indices Vs Wavelength of binary oxide thin films.

All the samples showed a constant value of refractive index throughout the region of 300-1100 *nm* (UV-Vis-NIR) and it clearly indicates that irrespective of variation in concentration, there exists a 'homogeneity' of the medium in each samples and thus reaffirms the uniformity in reducing the speed of light in the UV-Vis-NIR region. A low value of n=2. 4 was obtained for Q3 sample and a high refractive index of 2.8 was found for Q1 and Q4 (The reason for maximum value of refractive index particularly in Q1 and Q4 films was due to those samples has a high optical transmittance which is shown in transmittance spectrum) In particular, the higher values of the refractive index binary films suggest the application of the films in Opto-electronic industry shown in Fig. 4. This variation of refractive index may be due to the variation of packing density of the grains in the binary oxide samples.

3.3. Photoluminescence Analysis

In order to investigate the room temperature PL emission spectra of the TiO_2-MoO_3 binary films were subjected to excitation with the radiation of wavelength of 350 *nm*. The PL spectrum includes two prominent broad emissions corresponding to the wavelengths around 393 *nm* and 450 *nm* as shown in Fig. 5. In general, the emission spectra of semiconducting oxides can be classified into two categories: The near band edge emission (NBE) and the deep level (DL) emission, high crystal quality and the quantum confinement effect related to the nanostructures are two factors favoring the increase of intensity of UV emission at room temperature. Generally, if the energy of excitation light is greater than the band gap (Eg) of samples, hence the charge separation takes place (Production of electron-hole pair). The PL emission is the result of the recombination of excited electrons and holes, the lower PL intensity indicates the decrease in recombination rate, thus higher photocatalytic activity. Most of the electrons and hole recombination takes place within a few nanoseconds in the absence of scavengers. If the scavengers (such as Mo^{6+}) are present to trap the electrons and holes, the electrons and hole recombination can be suppressed, it leads to a photoluminescence quenching.

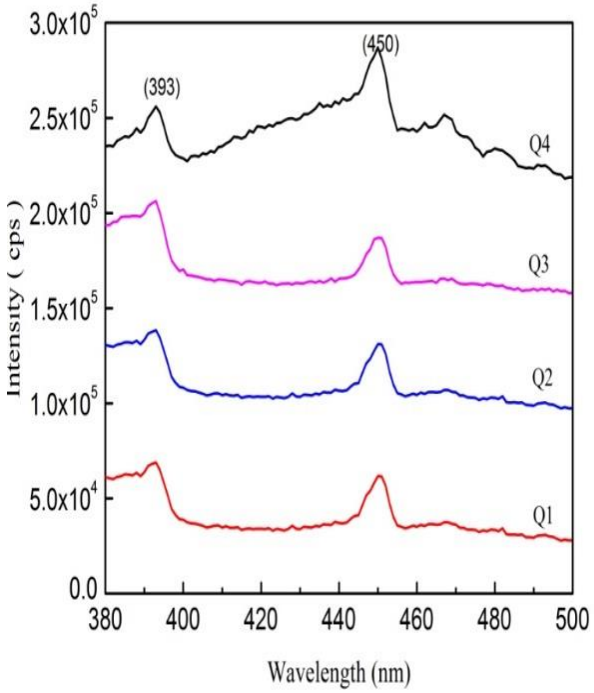

Fig. 5. Photoluminescence spectra of TiO_2-MoO_3 binary films.

3.4 Morphological and Elemental Analysis

SEM gives interesting results as shown in Fig. 6 to unfold certain surface morphological details which strongly depend on both the thickness and concentration of binary TiO_2-MoO_3 thin films coated on quartz substrates. The significant grain growth of binary oxide observed form SEM micrographs as an increase in concentration of MoO_3 which was confirmed by XRD analysis. The nanostructure of the films consisted of spherical shape grains, which is randomly distributed on the surface of lower concentration samples (in Q1 and Q2), upon increase in MoO_3concentration upto 0.25 M, grains were distributed throughout the surface, further increase in MoO_3 concentration the grains are bounded together to form floral structure as depicted in Q4 sample.

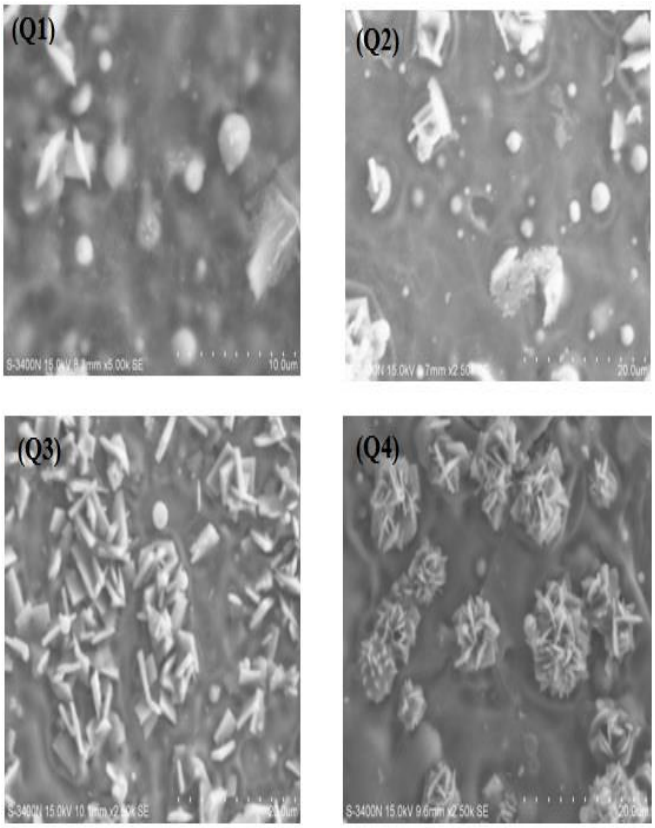

Fig. 6. Morphological properties of TiO_2-MoO_3 binary films.

Further, to confirm the microscopic understanding of the nature of interaction at the oxide / oxide level, the elemental composition of the deposited binary oxide thin films were examined by Energy dispersive X-ray analysis (EDAX) and shown in Fig. 7. The EDAX spectra confirm the existance of Mo, O and Ti and also the interface between the oxides. Moreover, similar trends in EDAX spectra were observed for other samples (Q2, Q3 and Q4) also.

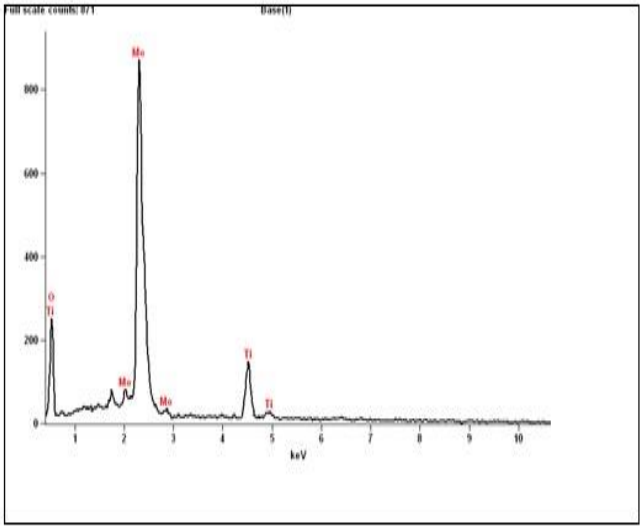

Fig. 7. EDX spectra of TiO_2-MoO_3 binary oxide thin film (Q1 sample).

3.5 Gas sensing Analysis

The gas sensing characteristics of binary (TiO_2-MoO_3) film were investigated by 100 ppm of ethanol at room temperature as shown in Fig. 8. It can be seen that, the resistance of the binary oxide thin film sensor decreased rapidly when the sensor exposed to ethanol gas and then recovered almost to the initial value while the ethanol gas supply was stopped and the air was introduced. The resistance of binary oxide film reduced when ethanol gas was introduced to chamber, this ethanol gas molecules were interacting with the chemisorbed oxygen species (O_2^-) occur in the surface of sensing compound, this reduction of resistance in the binary oxide films was due to the ethanol gas as the reducing gas, therefore the following equation (1) was explaining the interaction mechanism takes place in binary oxide sensor [25]:

$$2C_2H_5OH_{(gas)} + 2O_2^- \rightarrow 2CH_3CHO + 3H_2O_{(gas)} + 2e^- \quad (1)$$

The gas sensitivity of the binary TiO_2-MoO_3 films were estimated by the relation $S=R_{air}/R_{gas}$, where R_{air} is the resistance in the air atmosphere and R_{gas} is the resistance in the test gas present in the chamber. The gas sensitivity of the binary oxide sensor with respect to the MoO_3 concentration is depicted in Fig. 9, a maximum sensitivity was observed in Q3 sample and response and recovery time found to be 53 s and 41 s respectively. The reason for maximum response in Q3 sample was due to the matching of lowest unoccupied energy levels of the gas molecule with the interface energy (surface energy) of the film [26]. The response and recovery time of calculation and their variation are pictorially shown in Fig. 10 and Fig. 11.

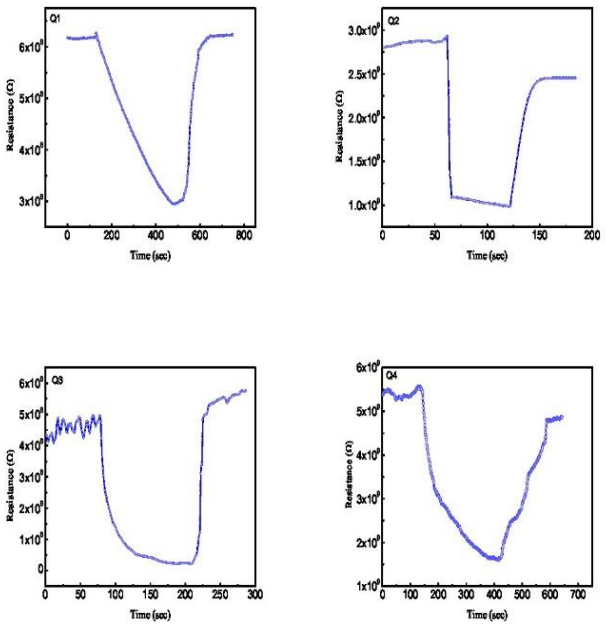

Fig. 8. Resistance Vs Time of TiO_2-MoO_3 binary films (Q1-Q4) towards 100ppm of ethanol at room temperature.

In general, the gas sensing mechanism can be influenced by many factors such as natural properties of base materials, surface areas and microstructure of sensing layers, surface additives, temperature and humidity etc., [27]. According to the influence factors on gas sensing characteristics of metal oxides, it is necessary to reveal the sensing mechanism of metal oxide gas sensor.

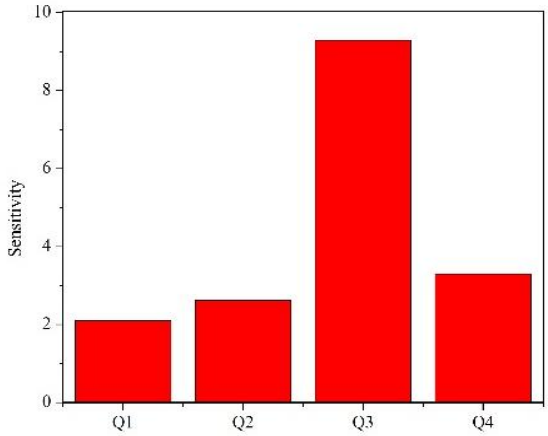

Fig. 9. Sensitivity of binary TiO_2-MoO_3 films.

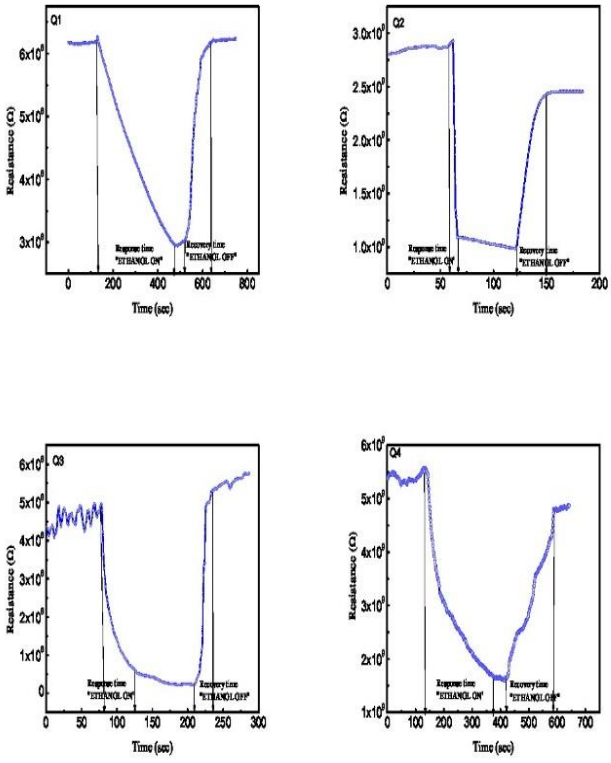

Fig. 10. Variation of resistance with respect to time of the samples Q1-Q4 which include Response and Recovery time.

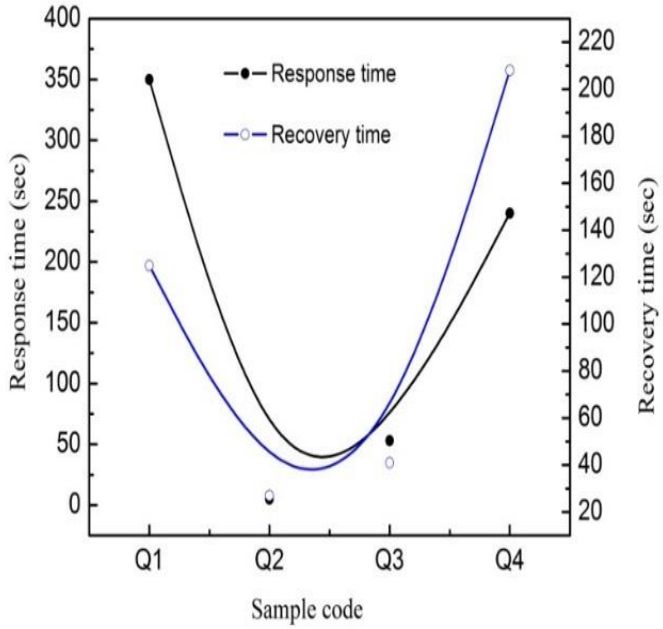

Fig. 11. Variation of Response and Recovery times of TiO_2-MoO_3 binary films (Q1-Q4).

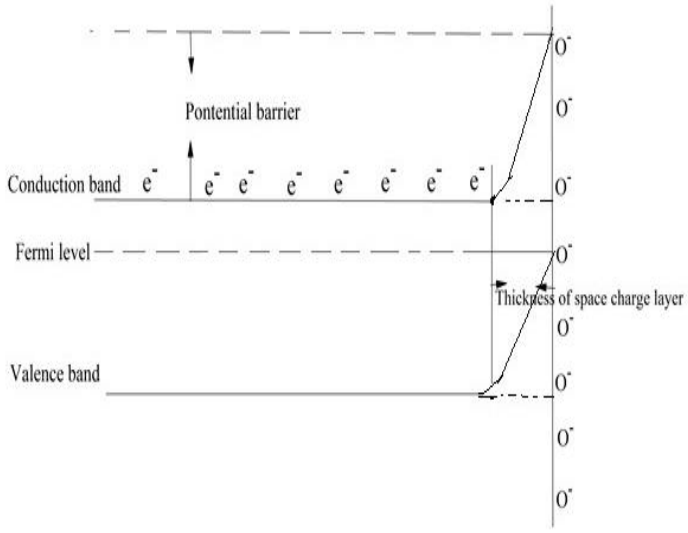

Fig. 12. Schematic diagram of band bending after chemisorptions of charged species.

The exact fundamental gas sensing mechanism that causes a gas response are still controversial, but essentially trapping of electrons at adsorbed molecules and band bending induced by these charged molecules is responsible for a change in conductivity. According to the band diagram (shown in Fig. 12), the adsorbed O_2 molecules on the surface of sensors, they would extract the electron from the conduction band and trap the electrons at the surface which is in the ions form. These ions are leading a band bending and an electron depleted region (space charge layer), which of thickness is the length of the band bending region. The adsorbed oxygen

species react with the gas molecules (as reducing gas) and replacement of the adsorbed oxygen by the other molecules decreases and can reverse the band bending, resulting in a decrement of resistivity.

4 Conclusion

In the present work, the physical and gas sensing properties of the binary TiO_2-MoO_3 thin films synthesized by a simplified spray pyrolysis technique (or perfume atomizer method) on quartz substrates have been discussed. The XRD studies confirmed that the formation of rutile titanium and orthorhombic molybdenum oxide thin films. The samples Q4 and Q1 showed a maximum optical transmission 25% at 1100 nm, other samples have poor transmission behavior**.** The parameters like refractive index and optical absorption coefficient were calculated from the transmission data and incorporated in the discussions. Further, the results of PL and SEM were taken into consideration in describing certain enhanced emissions at selective wavelengths and surface morphology. The elemental analysis confirmed the peaks corresponding to Mo, O and Ti atoms. As an application point of view, the gas sensing property of these binary oxide films was tested in ethanol gas environment as it has a pivotal role in many opto-electronic devices.

Acknowledgement

The authors (V.S and P.P) acknowledge the financial support provided by UGC New Delhi in the form of Rajiv Gandhi National Fellowship (F1-17.1/2011-2012/RGNF-SC-TAM-438/dt.06.06.2012) and MRP (F.No.41-961/2012 (SR) dt.26.07.2012).

References

[1] S.C. Navale, V. Ravi, I.S. Mulla, S.W. Gosavi and S.K. Kulkarni, *Sens. Actuators B,***126**, p382, (2007).

[2] M. Olvera, H. Gomez, and A. Maldonado, *Energy Mater. Sol. Cells*, **91**, p1449, (2007).

[3] A.B. Bodade, A.M. Bende and G.N. Chaudhary, *Vacuum*, **82**, p588, (2008).

[4] C. Rout, M. Hegde and C.N.R. Rao, *Sens. Actuators B*, **128**, p488, (2008).

[5] A.M. More, J.L. Gunjakar and C.D. Lokhande, *Sens.Actuator B: Chem*., **129**, p671, (2008).

[6] K. Bange, C.R. Otterrnann, O. Anderson, U. Jeschkowski, M. Laube and R. Feile, *Thin Solid Films*, 197, p279, (1991).

[7] Y. Sawada and Y. Taga, *Thin solid Films*, **116**, p155, (1984).

[8] T.L.Thompson and J.T.Yates, *Chemical Reviews*, **106**, p4428, (2006).

[9] A.Kubacka, G.Colo and M.Ferna´ndez-Garcı, *Catalysis Today*, **143**, p286, (2009).

[10] R.Subasri, M.Murugan, J.Revathi, G.V.N.Rao and T.N.Rao, *Materials Chemistry and Physics*,**124** (2010) p63.

[11] A.L.Castro, M.R.Nunes, M.D.Carvalho, L.P.Ferreira, J.-C. Jumas, F.M.Costa and M.H.Flor encio, *Journal of Solid State Chemistry*, **182**, p1838, (2009).

[12] T.Hitosugi,A.Ueda,S.Nakao,N.Yamada,Y.Furubaya shi,Y.Hirose, S.Konuma,T.Shimada and T.Hasegawa, *Thin SolidFilms*, **516**, p5750, (2008).

[13] C.M. Maghanga, G.A.Niklasson and C.G.Granqvist, *Thin Solid Films*, **518**, p1254, (2009).

[14] Y.Sato, H. Akizuki, T. Kamiyama and Y. Shigesato, *Thin Solid Films*, **516**, p5758, (2008).

[15] J.C. Volta, Proceedings of the 8th International Conference on Catalysts, (July 1984).

[16] E. Comini, K. Galatsis, Y. Li, W. Wlodarski, P. Siciliano A. Taurino and G. Sberveglieri, *INFM and dipartimento di chimica e fisica, via valotti***9**, 25133 Brescia, Italy.

[17] A. Taurine, M. Catalano, P. Siciliano, E. Comini and G. Sberveglieri, **92**, p286, (2003).

[18] Y. Sawada, C. Kobayashi, S. Seki, and H. Funakubo, *Thin Solid Films*, **409**, p46, (2002).

[19] K. Ravichandran and P. Philominathan,*Material Letters***62**, p2980, (2008).

[20] N. Balaguru and P. Philominathan, *International Journal of Renewable Energy Technology Research*, **9**, p208, (2013).

[21] N.Balaguru and P.Philominathan *International Journal of Current Research***5**, 3063-3068, (2013).

[22] E. G. Birgin, I. Chambouleyron, and J. M. Martnez, *Journal of Computational Physics*, p862, (1999).

[23] R. Swapna and M.C. Santhosh Kumar, *Journal of Physics and Chemistry of Solids***74**, 418–425, (2013).

[24] I. Hamberg and C.G. Granqvist, *Journal of Applied Physics*, **76**, p2740, (2000).

[25] IndumathyMuniyandi, Ganesh Kumar Mani, Prabakaran Shankar, John Bosco Balaguru andRayappan, *Ceramics International***40**, 7993–8001, (2014).

[26] Zeng Wen and LiuTian-mo, *Physica B*, **405**, 1345–1348, (2010).

[27] Chengxiang Wang, Longwei Yin, Luyuan Zhang, Dong Xiang and Rui Gao, *Sensors*, **10**, 2088-2106, (2010).